

# Experimental Design of the Multicolumn Countercurrent Solvent Gradient Purification (MCSGP) Unit for the Separation of PEGylated Proteins

Tae Keun Kim<sup>1</sup>, Chiara Botti<sup>1</sup>, James Angelo<sup>2</sup>, Xuankuo Xu<sup>2</sup>, Sanchayita Ghose<sup>2</sup>, Zheng Jian Li<sup>2</sup>, Massimo Morbidelli<sup>1</sup>, and Mattia Sponchioni<sup>1,\*</sup>

<sup>1</sup> Department of Chemistry, Materials and Chemical Engineering, Politecnico di Milano, Via Mancinelli 7, Milano, 20131, Italy

<sup>2</sup> Biologics Process Development, Global Product Development and Supply, Bristol Myers Squibb, Inc., Devens, MA, 01434, USA

\*Corresponding author: Mattia Sponchioni; E-mail: [mattia.sponchioni@polimi.it](mailto:mattia.sponchioni@polimi.it)

**Abstract:** *The rapid growth and diffusion of biopharmaceuticals, including polyethylene glycol (PEG)-protein conjugates, required to set up stringent regulatory requirements in terms of purity and clinical safety. In order to produce proteins that meet these requirements, the development of robust purification methods has been one of the main goals in the field of downstream processing in the last years. Most of these methods rely on single or sequential batch chromatographic separations, enabling to reach the purity specification but often at the expenses of low yield. An appealing alternative is the Multicolumn Countercurrent Solvent Gradient Purification (MCSGP). Thanks to the internal recycling of the fractions where product and impurities co-elute, this process can provide a significant improvement in the process yield, preserving the purity specification. The drawback lays in the increased number of process parameters compared to the batch, which complicates the design and optimization of this unit. In this work, we propose an ad hoc design procedure for the optimization of central-cut separations at a target purity. Using PEGylated lysozyme as a model system, we illustrate the use of this procedure to identify the load, the elution gradient as well as the collection intervals for optimal yield and productivity, at fixed purity specifications, for a batch (single) column system. The obtained optimal process parameters are subsequently transferred to the MCSGP unit. The so designed MCSGP process exhibited superior performances compared to the corresponding optimal batch process by increasing the yield and productivity by 17.0% and 2.1%, respectively, at the purity specification of 80%.*

**KEYWORDS:** Batch Purification; CIEX; IEX; MCSGP; PEG-lysozyme; Optimization

## 1. Introduction

In the biopharmaceutical industry, covalent conjugation of polyethylene glycol (PEG) to proteins is a common strategy to improve some of their characteristics that are critical for high therapeutic activity, including solubility, serum half-life, formulation property and immunogenicity<sup>1,2,3</sup>. Since the first approval of Adagen (PEG-adenosine deaminase; Sigma-Tau Pharmaceuticals, Inc.) and Oncaspar (PEG-L-asparaginase; Sigma-Tau Pharmaceuticals, Inc.), the global market of PEG-protein conjugates has reached USD 832.24 million in 2020 and is expected to reach USD 1.4 billion by 2025<sup>4</sup>. Covalent conjugation of PEG, or PEGylation, to proteins, peptides, oligonucleotides and small molecules has in fact shown proven safety and stability enhancement<sup>1,4</sup>.

The undoubted demonstration of clinical efficacy and safety is a mandatory requisite for a formulation to be released in the pharmaceutical market. For PEGylated proteins, this implies a careful purification of the target product, to be achieved through the recognition and separation of molecules with the wrong number of PEGs as well as the different positional isoforms<sup>5,25,27</sup>. For industrial production, this has increased the demand for robust chromatographic methods to exploit its unique purification efficiency and reach optimal yield<sup>5-7</sup>. One of the most common techniques used is ion exchange chromatography, as PEGylation leads to the alteration of the protein isoelectric point (pI) and in turn different electrostatic interactions with the stationary phase. Positional isomers of PEGylated proteins may have different strengths of electrostatic interactions, while an increased degree of PEGylation leads to more neutral pI, causing the elution at lower ionic strength in ion exchange chromatography<sup>5,8,9</sup>. Due to the high similarity of the chemical properties of the isoforms, a baseline separation of each species is rarely achieved in batch chromatographic purification<sup>11-15</sup>. In this case, overlapping regions of the target product and other impurities impose a trade-off between purity and yield. Broadening the collection interval, with the aim of improving the product yield, leads in fact to a higher amount of collected impurities, thus lowering the purity of the product pool. Vice versa, shortening the collection interval, with the aim of improving the product purity, leads to a decrease in the yield<sup>6,12,14,15</sup>. Although critical process parameters, such as the amount of product loaded onto a column as well as the slope and duration of the elution gradient can be optimized, a large amount of product is typically wasted with the product/impurities overlapping regions to satisfy the minimum requirement of purity, thus compromising the economic viability of the process<sup>16,17</sup>.

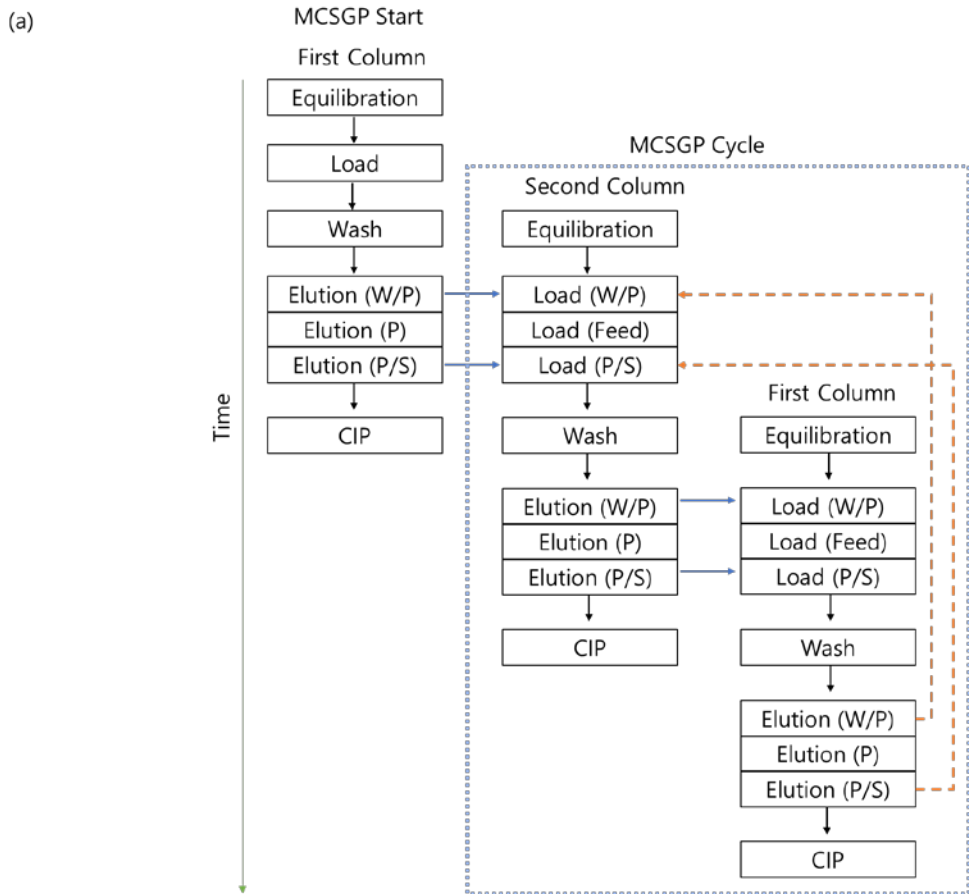
A valuable alternative to overcome this limitation of batch purification is offered by continuous operation, such as in the Multicolumn Countercurrent Solvent Gradient

Purification (MCSGP)<sup>12-23,26</sup>. In this continuous countercurrent purification technique, the overlapping peaks in the front (containing weakly bound impurities and product, hereinafter W/P region) and back (containing strongly bound impurities and product, hereinafter P/S region) of the target product are automatically recycled to a second column, in downstream position with respect to the loaded one, following an appropriate inline dilution<sup>21-23</sup>. In this way, the out of specification regions containing a significant amount of product are no longer discarded, as in the typical batch processes, thus minimizing the loss of yield while keeping the purity of the target product constant. The two identical columns of the MCSGP are synchronized and go through interconnected and disconnected operating modes as shown in the process flow diagram schematized in **Figure 1a**.

Since the operation of MCSGP units has been described already in detail<sup>15,17</sup>, we need here to briefly recall only some specific points relevant for this work. During the unit start-up, the first column undergoes the same sequence of operations: equilibration, loading, washing and CIP, as a typical batch operation, except for elution. The elution phase in the MCSGP operation is divided into three parts: recycle of the fraction W/P, pooling of P, and recycle of the fraction P/S. In the recycling parts, the first and second columns are interconnected to load the recycling fractions leaving the first column to the second one. Starting from the second column, that is from the second MCSGP cycle, similarly to the three-part elution phase, also the load phase consists of three parts: load of the W/P fraction, load of fresh feed, and load of the P/S fraction<sup>18,20-22</sup>. Following this internal recycling and fresh feed loading, the MCSGP cycles are repeated, one after the other, until reaching steady state conditions.

The difficulty in the optimal design of a MCSGP operation, as mentioned above, is in the large number of operating parameters compared to the batch process. In addition to the process parameters typical of the batch purification, including the two time values determining the pooling window, the optimization of a MCSGP accounts, in fact, for two additional degrees of freedom, *i.e.* the switching times between the interconnected phases and the product pooling window. With reference to the batch chromatogram in **Figure 1b**, the product pooling window is indicated as  $T_3$  and  $T_4$ , while  $T_2$  and  $T_5$  represent the times at which the product starts and ends eluting in the batch chromatogram, respectively. In the interconnected phases, the fractions within the intervals  $T_2$ - $T_3$  (W/P region) and  $T_4$ - $T_5$  (P/S region) have purity lower than the specification and then are internally recycled to the downstream column, while, in the disconnected phase, the fraction in the interval  $T_3$ - $T_4$  should have a purity higher than the specification so that it can be pooled. It is evident that an optimization strategy including, in addition to the amount of product loaded onto the column and the elution gradient, also the

switching times  $T_3$  and  $T_4$  is needed for reaching optimal MCSGP. For this, we start from an optimized batch purification - the so-called *design batch chromatogram* – which we consider as a convenient starting point towards optimal MCSGP conditions. In this work we focus on the procedure to identify such design batch chromatogram, with specific reference to loading of the target protein and slope of the modifier.



(b) First Column

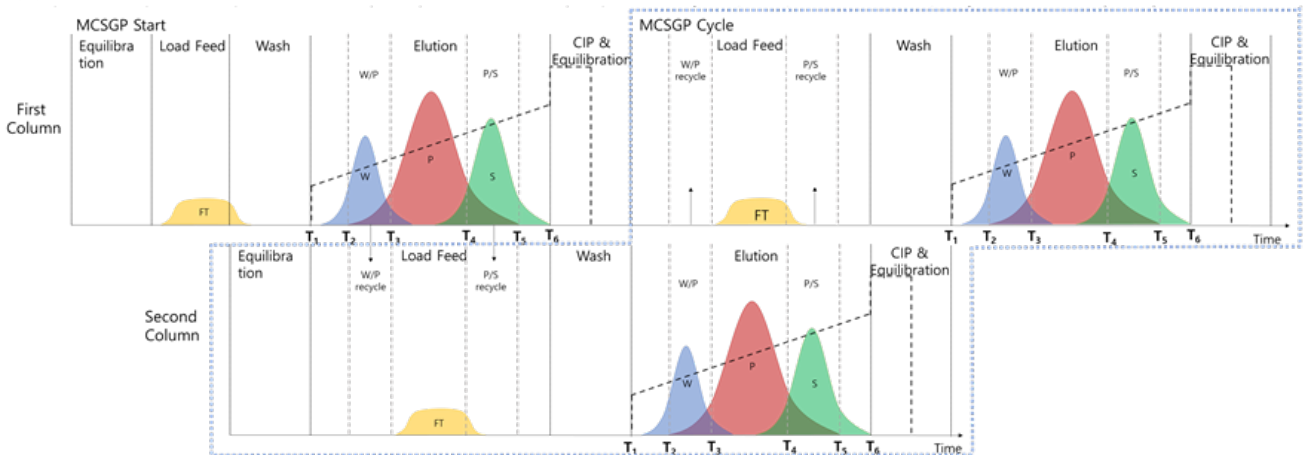


**Figure 1:** Schematic diagram of MCSGP operation. (a) Process flow diagram highlighting the different stages of the operation. Blue arrows indicate the interconnection and flow direction between the two columns. (b) Chromatogram of a typical central-cut purification. UV Peaks of flow through (FT ) , W () , P () , and S () are illustrated. The first row indicates the first column and the second row indicates the second column as labelled. The dashed straight line represents the equilibration buffer/elution buffer gradient.

Within this framework, in this work we first optimized the batch purification of PEGylated lysozyme (MW = 14,300 kDa), a well-known standard protein for chromatographic processes<sup>1,3-5</sup>. Next, based on such process conditions, we designed the optimal MCSGP. More in detail, using cation exchange chromatography in both preparative separations and analytics, different isoforms of PEG-lysozyme can be recognized and separated. We targeted a mono-PEGylated isoform of the protein as the desired product. On the other hand, multi-PEGylated proteins were collectively considered as weak impurities (W), while non-PEGylated lysozyme and different isoforms of the protein as strong impurities (S). For the batch process, we considered four optimization variables, namely the times of the pooling window  $T_3$ ,  $T_4$ , the slope of the modifier gradient slope and the loading amount, systematically varied to reach optimal yield and productivity at a fixed pool purity.

This is quite a complex task, particularly when considering an experimental not model based optimization process. For this we developed procedure based on a proper decomposition of the optimization problem leading in order to limit the experimental effort. Starting from a given loading and gradient slope, we changed  $T_3$  and  $T_4$  to reach optimal yield and productivity at the given purity specification. The procedure was then repeated for the same loading and different gradient slopes, comparing the optimal process performances found for each condition. Finally, the same procedure was applied to different loading times, thus determining the global optimum. This approach led to a robust, optimized batch design chromatogram that was considered as the starting point for the design of improved MCSGP operation. In particular, for the first time, we determined a Pareto front for yield and productivity of the MCSGP, at fixed product purity, with respect to the modifier gradient slope, loading and the switching times  $T_3$  and  $T_4$ .

## 2. Materials and Methods

### 2.1. Materials

Poly(ethylene glycol) methyl ether (mPEG,  $\geq 99\%$ , MW = 5,000, Sigma Aldrich), succinic anhydride (SA,  $\geq 99\%$ , MW = 100.07, Sigma Aldrich), 4-dimethylamino pyridine (DMAP,  $\geq 99\%$ , MW = 122.17, Sigma Aldrich), *N, N'*-dicyclohexylcarbodiimide (DCC,  $\geq 99\%$ , MW = 206.33, Sigma Aldrich), *N*-hydroxysuccinimide (NHS,  $\geq 99\%$ , MW = 115.09, Sigma Aldrich), Lysozyme from chicken egg white (Lys,  $\geq 99\%$ , MW = 14,300, Sigma Aldrich), Chloroform-d ( $\geq 99\%$ , MW = 120.38, Sigma Aldrich), dichloromethane (DCM,  $\geq 99\%$ , MW = 84.93, Sigma Aldrich), diethyl ether ( $\geq 99\%$ , MW = 74.12, Sigma Aldrich), ((2-(*N*-Morpholino)ethanesulfonic acid hydrate (MES,  $\geq 99\%$ , MW = 195.24, Sigma Aldrich), sodium chloride (NaCl,  $\geq 99\%$ , MW = 58.44, Sigma Aldrich), sodium hydroxide (NaOH,  $\geq 99\%$ , MW = 40.00, Sigma Aldrich), sodium phosphate monobasic anhydrous (NaPi monobasic,  $\geq 99\%$ , MW = 119.98, Sigma Aldrich), sodium phosphate dibasic anhydrous (NaPi dibasic,  $\geq 99\%$ , MW = 141.96, Sigma Aldrich), hydrochloric acid 37% (HCl,  $\geq 99\%$ , MW = 36.46, Sigma Aldrich) MiniChrom Column Eshmuno CPX (CPX column, 8 × 100 mm, Merck), ProPac WCX-10 (WCX column, 4 × 250 mm, Thermo Scientific), deionized water (DW, Merck Millipore) were used for experimentations. All buffers were filtered with 0.22  $\mu\text{m}$  cellulose-acetate filters (Merck Millipore) and degassed for chromatographic purposes.

### 2.2. PEGylation of Lysozyme

Amine conjugation is selected for the covalent binding of lysozyme to mPEG<sup>24</sup>. The conjugation method consists of conversion of mPEG to mPEG-carboxylic acid, activation of the carboxylate group to succinimidyl ester (mPEG-NHS), and conjugation of mPEG-NHS to lysozyme<sup>24</sup>. In the first step of the conjugation method, 10 g of mPEG (2 mmol, 1 eq), 0.26 g succinic anhydride (2.6 mmol, 1.3 eq), and 54 mg of DMAP (0.44 mmol, 0.22 eq) were mixed in 40 g of DCM at room temperature overnight. The mixture was then precipitated in 250 mL of diethyl ether and vacuum-dried for an hour. In the second step, 8 g of mPEG-carboxylic acid (1.57 mmol, 1 eq), 0.22 g of NHS (1.88 mmol, 1.2 eq), and 0.39 g of DCC (1.88 mmol, 1.2 eq) were mixed in 40 g of DCM at room temperature overnight. Using sintered glass filtration, the white precipitate of dicyclohexylurea was discarded, and with the same precipitation method used in the first step, the filtered mixture was precipitated as mPEG-NHS. In the last step of the conjugation, 6.86 g of lysozyme were dissolved in 1.37 L of 25 mM sodium phosphate buffer (pH 7.0) and then 3 g of mPEG-NHS were added to the buffer.

After mixing for at least 1 h, mPEG-lysozyme was filtered with cellulose-acetate filters and stored at 4 °C. An amount of 0.05 g of each of the process intermediates, mPEG-carboxylic acid and mPEG-NHS, were dissolved in 1 mL of deuterated chloroform and analyzed using proton nuclear magnetic resonance (<sup>1</sup>H NMR) spectroscopy performed on a Bruker 400 MHz spectrometer, with 64 scans per sample.

### 2.3. Batch Purification of PEGylated Lysozyme

The separation of mono-PEGylated lysozyme from multi-PEGylated lysozyme and non-reacted lysozyme was performed on a ContiChrom CUBE Combined (ChromaCon), using an Eshmuno CPX column 8 × 100 mm (column volume (CV) = 5.024 mL). Equilibration buffer (20 mM sodium phosphate, pH 6.1), Elution buffer (25 mM sodium phosphate, 500 mM sodium chloride, pH 6.1), Strip buffer (25 mM sodium phosphate, 1000 mM sodium chloride, pH 6.1), and CIP buffer (500 mM sodium hydroxide) were filtered with 0.22 μm filters before use. A summary of the batch run operating conditions are summarized in **Table 1**. The process was conducted at constant flow rate of 300 cm/h with different column volumes (CVs) of the different steps. In the elution phase, the gradient starts from 90% equilibration buffer/10% elution buffer and linearly goes to 40% equilibration buffer/60% elution buffer over the given CVs, and 30 fractions were collected. The chromatogram was recorded by measuring the UV absorbance at 280 nm.

**Table 1:** *Batch operation for PEG-lysozyme purification*

Phase	Volume (CV)	Remarks
Equilibration	3.0	Equilibration buffer
Load Feed	3.0, 4.0, 7.7 <sup>(1)</sup> , 60.0 <sup>(2)</sup>	mPEG-lysozyme (5 g/L) 60 Fractions for breakthrough experiment <sup>(3)</sup>
Wash	3.0	Equilibration buffer
Elution	5.0, 8.0, 10.0, 12.0, 15.0 <sup>(1)</sup>	Elution buffer 10% to 60% linear elution gradient 30 Fractions
Strip	2.0	Strip buffer
CIP	2.0	CIP buffer
Re-Equilibration 1	1.0	Elution buffer
Re-Equilibration 2	3.0	Equilibration buffer

<sup>(1)</sup>Each load volume was tested with each elution volume except for 60 CV load feed phase

<sup>(2)</sup>Volume used for the breakthrough experiment

<sup>(3)</sup>Load feed fractionation is carried out only for the breakthrough test

#### 2.4. Analytic Chromatography

mPEG-lysozyme from Section 2.2 and fractions from the CPX chromatography were analyzed by cation exchange high performance liquid chromatography (HPLC) using a ProPac WCX-10 column (4 × 250 mm). MES A buffer (20 mM MES, pH 5.5) and MES B buffer (20 mM MES, 500 mM sodium chloride, pH 5.5) were filtered with 0.22 μm filters and degassed under vacuum. The analysis is performed on an Agilent 1100 series HPLC at 1 mL/min and room temperature, following the buffer composition program reported in **Table 2**. The absorbance was measured at 280 nm using a diode-array detector. The purity of a fraction could be computed by the ratio of the area of the target product ( $Area_{target}$ ) and the total area of the fraction analyzed ( $Area_{total}$ ):

$$Purity = \frac{Area_{target}}{Area_{total}} \times 100\% \quad (1)$$

With a given product pool, recovery of the target product, or yield, could be calculated by the ratio of the mass of the target product collected within the product pool ( $m_{recovered}$ ) and the mass of the total target product loaded onto the column ( $m_{total}$ ):

$$Yield (\%) = \frac{m_{recovered}}{m_{total}} \times 100\% \quad (2)$$

Using the total time for a batch purification,  $T_{total}$  given by **eq.3**, and the CV value, productivity was calculated as follows:

$$T_{total} = T_{EQ} + T_{Load} + T_{Wash} + T_{Elu} + T_{Strip} + T_{CIP} + T_{ReEQ1} + T_{ReEQ2} \quad (3)$$

$$Productivity = \frac{m_{recovered}}{CV \times T_{total}} = \frac{C_{feed} \times Q_{feed} \times T_{Load}}{CV \times T_{total}} \times Yield \quad (4)$$

**Table 2:** WCX-HPLC analytical method

Time (min)	MES B (%)
0.00	20
5.00	20
5.01	30
9.00	25
9.01	5
17.00	50

17.01	100
18.50	100
18.51	3
23.00	3

## 2.5. Optimal Design Procedure for the Batch Operation

As mentioned above, in the developed optimal batch design procedure, we considered, as optimization parameters, the load amount of the feed and the elution gradient slope. The first one is represented in the following, for a fixed composition of the feed, by the loading time,  $T_{load}$ , while the second is described by the elution time with fixed extremes of the gradient (10% and 60% elution buffer, respectively),  $T_{elu}$ . Now, as  $T_{load}$  increases and  $T_{elu}$  decreases, purity decreases, due to the enlarged W/P and P/S regions, but potentially productivity increases as shown in **eq.4**. Yield is strictly related to the purity specification,  $P_{spec}$ , and of course higher yield values can be achieved for less stringent purity specifications.

In this work, we developed an optimization procedure considering yield and productivity as the output performance parameters, with the constraint of the purity being within specifications, i.e.,  $P \geq P_{spec}$ . With illustrative purposes we considered two  $P_{spec}$  values, 80% and 90%, representative of two relevant practical situations. Four optimization variables were considered:  $T_3$ ,  $T_4$ ,  $T_{elu}$  and  $T_{load}$ , while all the other process operating parameters were kept constant.

In the first step of the experimental procedure, from a single batch purification, at given  $T_{elu}$  and  $T_{load}$ , 30 fractions within the elution phase were collected and analyzed *via* HPLC, thus leading to a batch chromatogram such as the one shown in Figure 1b as well as the purity and amount of recovered product in each sample. We then selected various  $T_3$  values in the range  $T_2$ - $T_5$ , and for each of them we evaluated the purity, yield and productivity of hypothetical product pools (interval  $T_3$ - $T_4$ ) obtained by increasing  $T_4$  from  $T_3$  to  $T_5$ , and retaining only those respecting the purity specification, i.e.,  $P \geq P_{spec}$ . The optimal pair ( $T_3$ ,  $T_4$ ), for a given  $T_{elu}$  and  $T_{load}$ , was taken as the one leading to the maximum yield, which also corresponds to the one leading to the maximum productivity since, as evident from **eq. 4**, when  $T_{total}$  is fixed, these two performance parameters are directly correlated.

The same procedure was then repeated, at a fixed  $T_{load}$ , for different values of  $T_{elu}$ , namely 10.0, 16.0, 20.0, 24.0, and 30.0 min (*i.e.* 5.0, 8.0, 10.0, 12.0, and 15.0 CVs, in **Table 1**). For each value of  $T_{elu}$ , the optimal pair ( $T_3$ ,  $T_4$ ) leading to maximum yield and productivity and

ensuring  $P \geq P_{\text{spec}}$  was determined. The obtained values were then compared for determining the optimal conditions  $T_3$ ,  $T_4$  and  $T_{\text{elu}}$  for the selected  $T_{\text{load}}$  value.

Finally, the procedure was repeated for different values of  $T_{\text{load}}$ , namely 6.0, 8.0, and 15.4 min (*i.e.* 3.0, 4.0, and 7.7 CVs) and the corresponding optimal conditions were compared to define the global optimum. In this analysis, an upper limit for  $T_{\text{load}}$  was imposed in order to avoid breakthrough during the loading step. For this, a breakthrough experiment was preliminary performed by loading 60 CVs of feed onto the column. The dynamic binding capacity (DBC) for the weak impurities, which are the species breaking through the column earlier in the process, was determined as the amount of protein loaded at 10% breakthrough of the impurities. The upper limit for  $T_{\text{load}}$  was determined as the time required to load 70% of the weak impurity DBC, hereinafter referred to as the operating binding capacity (OBC). As discuss later, the batch purifications with  $T_{\text{load}} = 8.0$  min and  $T_{\text{elu}} = 10.0, 20.0, \text{ and } 30.0$  min were eventually selected to be implemented into the MCSGP.

## 2.6. MCSGP Operation

The buffers and operating parameters of the batch purification can be directly translated to the MCSGP with proper modifications of the loading and elution phases, due to recycling of the target product-impurity overlaps during the interconnected operating phase<sup>12-21</sup>. The modifications are required for inline dilution of the W/P and P/S regions. Since the modifier decreases the affinity of the proteins towards the solid phase, dilution by the equilibration buffer, to lower the modifier concentration of the W/P and P/S fractions recycled to the downstream column, is done to avoid early elution. In order to start-up the MCSGP unit, we apply to the first column the same equilibration and loading phases of the batch purification as shown in **Table 1**. After loading, the first column proceeds to the regeneration and re-equilibration phases as shown in **Table 3**, while the second column follows the first step from **Table 3**, so that there is a half-cycle shift between the two columns. In the elution phase of the first column, the W/P, target product, and P/S fractions are eluted at different flow rates. During the recycle of W/P and P/S, the columns are interconnected and the elution of the recycled fractions of the first column becomes a partial feed to the second column, with the inline dilution by the equilibration buffer. After the elution phase of both columns, the first cycle of the MCSGP is completed, and two fractions are collected, one from each column as illustrated in **Figure 2**. Considering the start-up for the first column, running 5 cycles of the MCSGP produces 11 fractions. Yield and productivity were computed according to **eq. 5** and

eq. 6, respectively.  $T_{load}$  per switch of the first switch was 8.0 min, while  $T_{load}$  per switch of the remaining switches were 5.8 or 7.5 min as shown in the load phase of **Table 3**.

$$Yield (\%) = \frac{m_{recovered\ per\ switch}}{m_{total\ per\ switch}} \times 100\% \quad (5)$$

$$Productivity = \frac{m_{recovered\ per\ switch}}{CV \times T_{total\ per\ switch}} = \frac{C_{feed} \times Q_{feed} \times T_{Load\ per\ switch}}{CV \times T_{total\ per\ switch}} \times Yield \quad (6)$$

**Table 3: MCSGP operation for mPEG-lysozyme purification**

Phase	Volume (CV)	Flow rate (cm/hr)		Remarks
Equilibration	3.0	300.0		Equilibration buffer
Load Feed	0.2 <sup>(1)</sup> , 0.1 <sup>(2)(3)</sup>	Inline dilution: 223.6 <sup>(1)</sup> , 199.8 <sup>(2)</sup> , 186.6 <sup>(3)</sup>	W/P recycle: 76.4 <sup>(1)</sup> , 100.2 <sup>(2)</sup> , 113.4 <sup>(3)</sup>	mPEG-lysozyme (5 g/L) W/P and P/S: Interconnected mode in which the impurity-product recycles come from Elution phase of the second column
	2.9 <sup>(1)</sup> , 3.8 <sup>(2)(3)</sup>	300.0		
	0.9 <sup>(1)</sup> , 0.2 <sup>(2)(3)</sup>	Inline dilution: 240.3 <sup>(1)</sup> , 229.6 <sup>(2)</sup> , 224.8 <sup>(3)</sup>	P/S recycle: 59.7 <sup>(1)</sup> , 70.4 <sup>(2)</sup> , 75.2 <sup>(3)</sup>	
Wash	3.0	300.0		Equilibration buffer
Elution	5.0 <sup>(1)</sup> , 10.0 <sup>(2)</sup> , 15.0 <sup>(3)</sup>	W/P recycle: 76.4 <sup>(1)</sup> , 100.2 <sup>(2)</sup> , 113.4 <sup>(3)</sup>		Elution buffer 10% to 60% linear elution gradient 1 Fractionation W/P and P/S: Interconnected mode in which the impurity-product recycles are loaded onto the second column
		119.3 <sup>(1)</sup> , 210.0 <sup>(2)</sup> , 300.0 <sup>(3)</sup>		
		P/S recycle: 59.7 <sup>(1)</sup> , 70.4 <sup>(2)</sup> , 75.2 <sup>(3)</sup>		
Strip	2.0	300.0		Strip buffer
CIP	2.0			CIP buffer

Re-Equilibration 1	1.0		Elution buffer
Re-Equilibration 2	3.0		Equilibration buffer

(1) 5 CV Elution

(2) 10 CV Elution

(3) 15 CV Elution

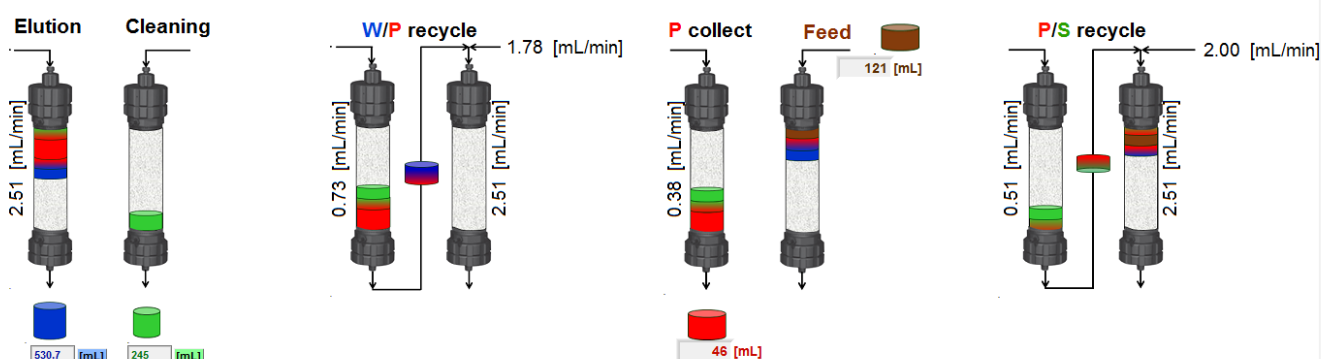


**Figure 2:** Schematic diagram of 5 CV elution gradient MCSGP operation.

### 3. Results and discussion

#### 3.1. Synthesis of mPEG-Lysozyme and its Intermediates

The PEGylated lysozyme was synthesized according to the reaction pathway reported in **Figure S1a** (see Supporting Information section). This procedure involves the functionalization of mPEG with a carboxyl group, its activation with NHS and the final conjugation to lysozyme. The degree of functionalization for each step was determined through  $^1\text{H}$  NMR spectroscopy. The spectrum of mPEG-carboxylic acid is shown in **Figure S1b**. The peak attributed to succinic acid appears at 2.56 ppm and from its integration the degree of functionalization was calculated according to **eq. S1** and it was equal to 94%. This intermediate was then activated through the nucleophilic addition of NHS. The conversion in this case was calculated from the  $^1\text{H}$  NMR spectrum reported in **Figure S1c** by comparing the peak of NHS at 2.83 ppm to the one attributed to PEG (**eq. S2**), which led to a conversion of 81%. Finally, the activated PEG-NHS was contacted with lysozyme in a sodium phosphate buffer (25 mM, pH 7.0) for the PEGylation of the protein.

As it usually the case for all PEGylations, this process led to a variety of species, comprising multi-PEGylated, mono-PEGylated, and unreacted lysozyme. To analyze the reaction

product, which represents the feed of the chromatographic separation, weak cation exchange (WCX) HPLC was used. The separation of the different species of mPEG-lysozyme is shown in the chromatogram reported in **Figure 3**. In this chromatogram, five peaks are separated and labeled with the corresponding elution time. W indicates the weak impurities, that is the multi-PEGylated lysozyme species which tend to bind the weakest to cation exchange resins. P and S indicate product and strong impurity, respectively, and are positional isomers of mono-PEGylated lysozyme. For this study, only P was arbitrarily chosen as the target product in subsequent analyses, in order to test the optimization procedure described above. Finally, the species eluting at 19.8 min is the unreacted lysozyme. From the chromatogram, areas of each peak can be integrated to evaluate the proportions of the feed. The areas of W, P, S, and unreacted lysozyme were 1138.6, 2374.0, 2287.1, and 5917.2 [mAU × min], respectively, and their proportions were 9.7, 20.3, 19.5, and 50.5%, respectively. The peak area information is summarized in **Table 4**. From the integration of the chromatogram, the product purity in the feed was determined as 20.3%, which is in general too low for biomedical applications.

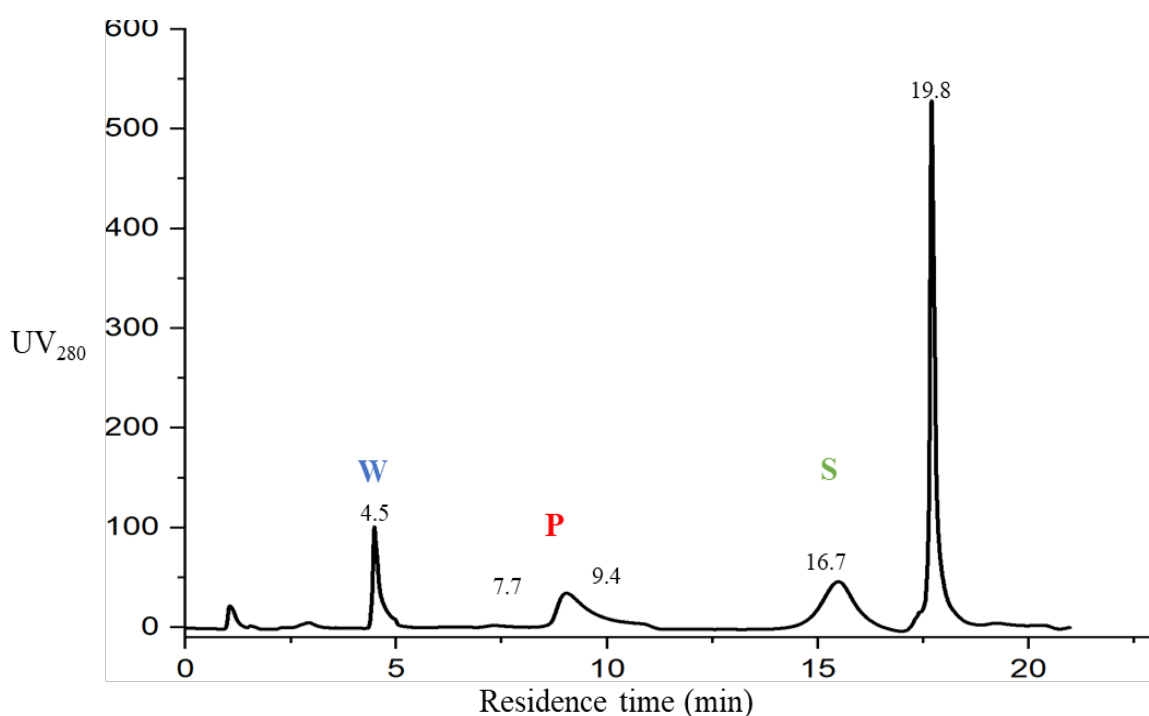


**Figure 3:** Chromatogram of mPEG-lysozyme using WCX-HPLC

**Table 4:** Peak analysis of mPEG-lysozyme chromatogram

Species	Residence time (min)	Area (mAU×min)	Composition (%)	Concentration (C <sub>species</sub> , g/L) <sup>(1)</sup>
---------	----------------------	----------------	-----------------	---

Weak impurity	4.5	1138.6	9.7	0.49
Product	7.7	2374.0	20.3	1.01
Strong impurity	16.7	2287.1	19.5	0.98
Unreacted lysozyme	19.8	5917.2	50.5	2.53

<sup>(1)</sup>Total concentration equal to 5 g/L

### 3.2. Breakthrough Test of Eshmuno CPX Column

Determination of dynamic binding capacity (DBC) and operating binding capacity (OBC) of a column is necessary in running chromatography as loss of target product during the loading phase may alter elution profiles and intrinsically decrease the maximum yield achievable. DBC is the maximum amount of target product that can be loaded onto a column at a given allowed breakthrough, which typically varies from 1 to 10% of its concentration in the feed ( $C_{\text{species}}$ ). In this experiment, the allowable breakthrough point was set at 10%, and thus the volume at which each species reaches its 10% breakthrough ( $V_{10\%BT}$ ) was measured to compute the DBC according to **eq. 7**.

$$DBC = \frac{C_{\text{Species}} \times V_{10\%BT}}{CV} \quad (7)$$

OBC is a safety margin of DBC to prevent any loss of the target protein, which was set at 70% of DBC in this work. As shown in **Table 1**, during the loading phase, 60 CVs of feed, or 1507.2 mg of mPEG-lysozyme, were loaded onto the column in 120 min ( $C_{\text{feed}} = 5 \text{ g/L}$ ,  $T_{\text{load}} = 120 \text{ min}$ ). A total of 60 fractions, each one lasting two min, were collected during the loading and analyzed *via* HPLC. The measured concentration values are shown in **Figure 4** for the different species. As expected, at 100% breakthrough the eluate composition is equal to that of the feed. As reported in **Table 4** the corresponding concentration values for weak impurity, target product, strong impurity and unreacted lysozyme corresponded to 0.49, 1.01, 0.98, and 2.53 g/L, respectively. The competitive binding for the different species is evident from the results shown in the figure. In particular, when the binding sites are saturated, the product displaces the weak impurity for binding. This justifies the overshoot in the weak concentration in the eluate compared to the feed. In fact, the weak impurity previously adsorbed onto the column is replaced by the more strongly adsorbed P and S and from this point on, the W loaded with the feed elutes without binding to the column. The same fate is experienced by P and S, which are displaced by the even more strongly adsorbed unreacted lysozyme. Again, the overshoot in P and S concentrations indicate the desorption of such species from the resin,

until all of the binding sites are saturated by the unreacted lysozyme and P and S flow through the column without binding.

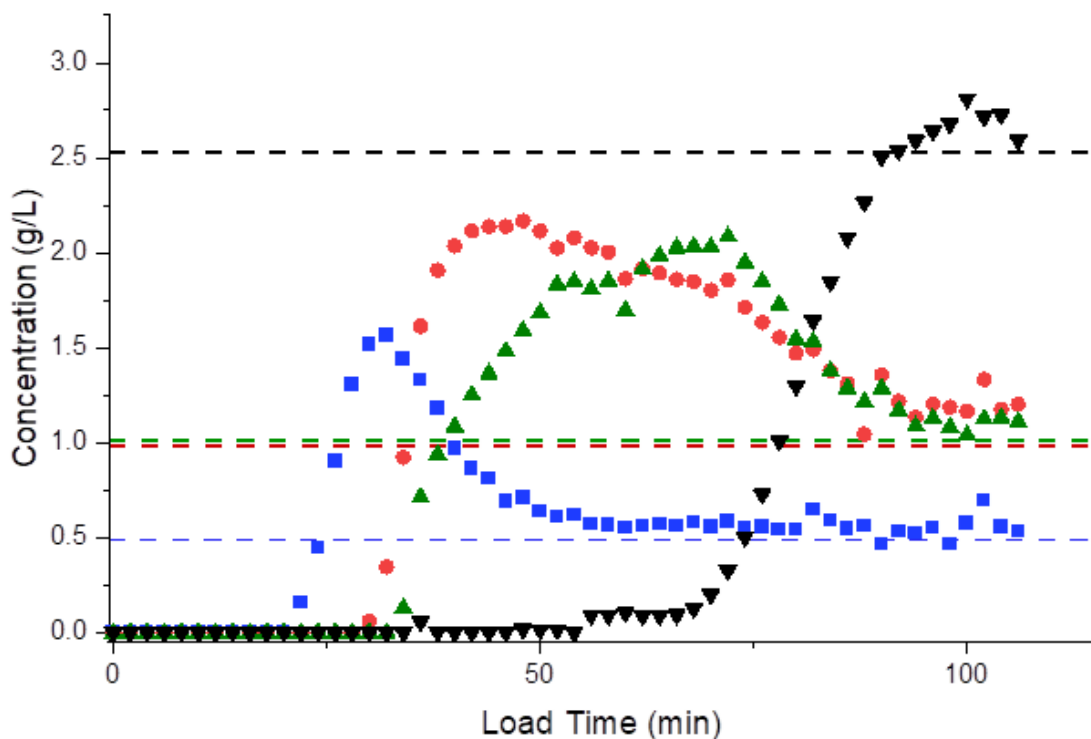


**Figure 4:** Eluate composition of the fractions collected during the loading of 1507.2 mg of the PEGylated lysozyme onto the Eshmuno CPX column for the breakthrough test. The concentration of W (■), P (●), S (▲), and lysozyme (▼) are determined via WCX-HPLC. The dashed horizontal straight lines indicate the feed concentration of the different species.

The 10% breakthrough points of W, P, S, and lysozyme were reached at  $T_{load} = 22, 34, 38,$  and  $86$  min corresponding to loading equal to  $V_{10\%BT} = 55.26, 85.41, 95.46,$  and  $216.03$  mL, respectively. Using **eq. 7**, the  $DBC_{10\%BT}$  values of  $5.34$   $\text{mg}_{weak}/\text{mL}_{resin}$ ,  $17.22$   $\text{mg}_{product}/\text{mL}_{resin}$ ,  $18.54$   $\text{mg}_{strong}/\text{mL}_{resin}$ , and  $108.58$   $\text{mg}_{lys}/\text{mL}_{resin}$ , reported in **Table 5** for each species were computed. A zoomed-in chromatogram of the loading phase is shown in **Figure S2**, and the blue vertical straight lines indicate the loading times at which each specie reaches its  $DBC_{10\%BT}$ . As mentioned above, the maximum loading in the batch purification was taken equal to the  $OBC_{weak}$ , resulting in the maximum  $T_{load}$  equal to 15.4 min.

**Table 5:**  $DBC_{10\%BT}$  of the different species

Species	Loading time	Load volume	$DBC_{10\%BT}$
---------	--------------	-------------	----------------

	( $T_{\text{load}}$ , min)	( $V_{\text{DBC}}$ , mL)	(mg <sub>species</sub> /mL <sub>resin</sub> )
Weak impurity	22	55.26	5.34
Product	34	85.41	17.22
Strong impurity	38	95.46	18.54
Unreacted lysozyme	86	216.03	108.58

### 3.3. Optimal Design of the mPEG-Lysozyme Batch Purification

In the optimization of the batch purification, we imposed the constraint on purity such that  $P \geq P_{\text{spec}}$ , while yield and productivity were considered as process performance parameters. On the other hand, the optimization variables were  $T_{\text{load}}$ ,  $T_{\text{elu}}$ , and the collection interval, defined by the times  $T_3$  (collection start) and  $T_4$  (collection end). In principle, this interval can be set between  $T_2$ , at which the target product starts to elute, and  $T_5$ , at which the target product is completely eluted, as sketched in **Figure 1b**.  $T_{\text{load}}$  and  $T_{\text{elu}}$  have a direct impact on productivity as they are included in the total duration of the batch run, or  $T_{\text{total}}$ , as shown in **eq. 4**. At the same time,  $T_{\text{load}}$  has an impact on the amount of the target product loaded. The collection interval  $T_3$ - $T_4$ , instead, mainly affects the product yield and of course its purity. Two values of  $P_{\text{spec}}$ , 80% and 90%, were considered in this study for illustrative purposes. As mentioned in **Table 1**, three different  $T_{\text{load}}$ , 6.0, 8.0, and 15.4 min, and five different  $T_{\text{elu}}$ , 10.0, 16.0, 20.0, 24.0, and 30.0 min, were selected as the range of the input process parameters. The operational points were chosen starting from a validated batch chromatogram allowing a suitable separation of the three main components, corresponding to  $T_{\text{load}} = 6.0$  min and  $T_{\text{elu}} = 20$  min.  $T_{\text{load}}$  was then augmented for evaluating the performances in the case of increased overlaps of W/P and P/S and the trade-off between yield and productivity by increment of 1 CV of load, equivalent to  $T_{\text{load}} = 8.0$  min, and up to its maximum load, which was equivalent to  $T_{\text{load}} = 15.4$  min, to represent the worst case for the separation. The range of  $T_{\text{elu}}$  was from 10 to 30 min for the worst case and best case, respectively, and two more  $T_{\text{elu}}$  were selected mid-points between each worst/best case to the center point, for the evaluation of the overlaps. First, we fixed  $T_{\text{load}} = 6.0$  min and  $T_{\text{elu}} = 20$  min. **Figure 5a** shows the chromatogram of the batch purification in these conditions. During the elution phase of the chromatogram, from 18.5 to 38.5 min, three distinct peaks were observed. The first one, from 20.0 to 25.0 min corresponds to the weak impurity, W, the second peak from 25.0 to 32.0 min to the target product, P, and the last peak from 32.0 to 41.0 min to the strong impurity, S. A fourth peak, the largest one, is observed at 42.0 min, corresponding to the unreacted lysozyme. This chromatogram was obtained with a gradient of the buffer conductivity, obtained by linearly

increasing the fraction of elution buffer. As the nomenclature of the impurities indicated, the weak impurity was bound the weakest to the column due to its di-PEGylated form that decreases its affinity to the cation exchanger. The target product and strong impurity are positional isomers of mono-PEGylated lysozyme, and the separation between the two isoforms indicates that the PEGylation site impacts significantly the binding affinity. 30 fractions were collected during the elution phase, as shown by the vertical lines labelled from 1 to 30 in the chromatogram. It is seen that a certain portion of the product peak overlaps with the W peak in the front and with the S peak in the rear. It is therefore evident that, in batch chromatography, these overlapping regions should be discarded for reaching the requested  $P_{spec}$ , thus leading to a significant loss in the product yield.

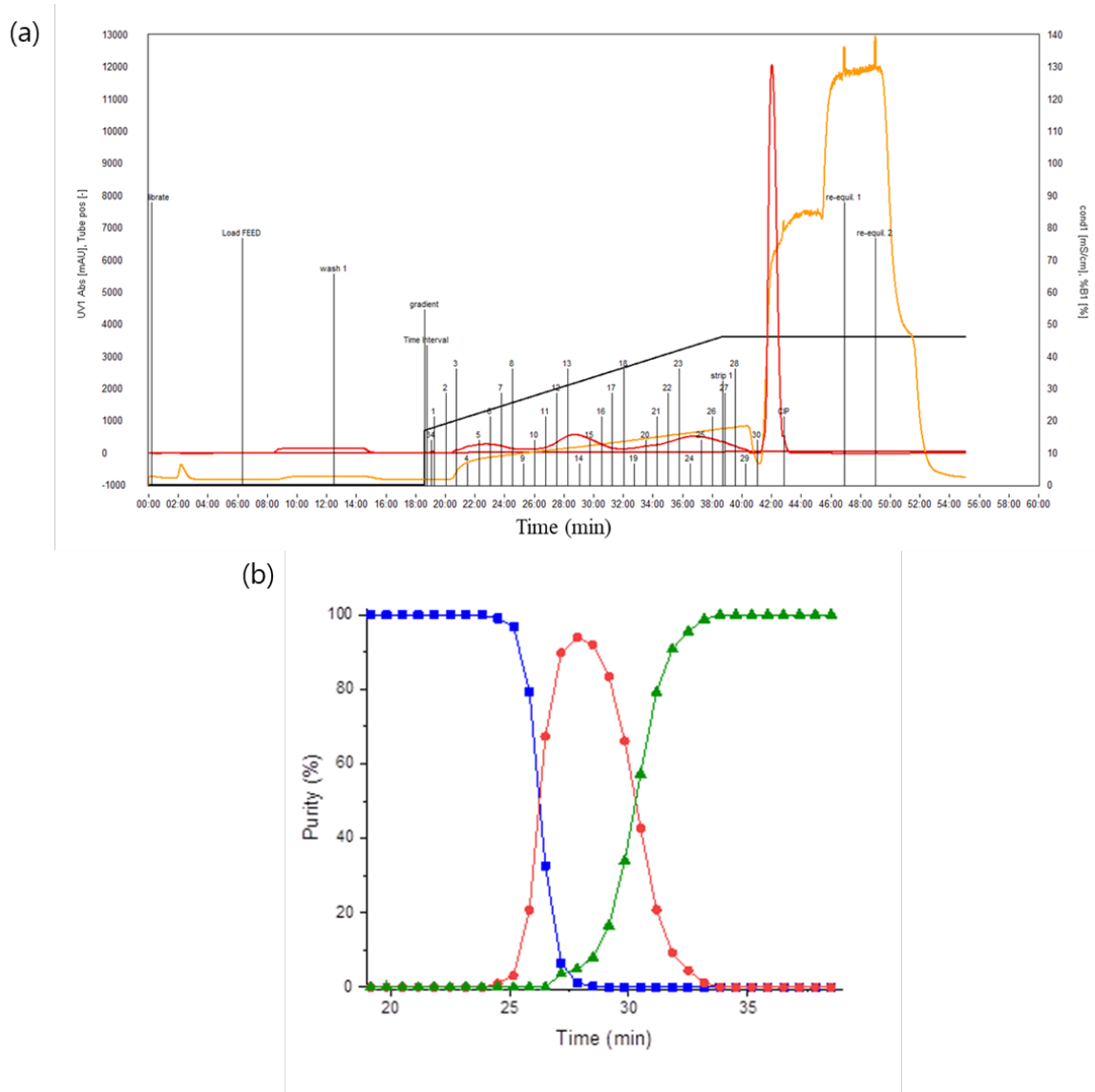


**Figure 5:** (a) CPX chromatogram of the batch purification of mPEG-lysozyme ( $T_{load} = 6.0$  min and  $T_{elu} = 20.0$  min). UV absorbance at 280 nm (■), conductivity (■), and %elution

buffer (■) are displayed. The vertical straight lines shown during the gradient indicate the number of fractions. (b) Elution profile of the batch purification of mPEG-lysozyme. The purity of W (■), P (●), S (▲), and lysozyme (▼) are determined via WCX-HPLC.

The 30 fractions collected were analyzed *via* off-line HPLC to evaluate the concentration of the different species. As shown in **Figure 5b**, only the weak impurity was found in the first 8 fractions going from 18.5 to 23.8 min. From 23.8 min, P started eluting, so we considered this point as  $T_2$ . The P elution lasted until 33.2 min, and this was taken as  $T_5$ .

With reference to the target product, we considered different hypothetical collection intervals from  $T_3$  to  $T_4$ . A total of 30 values of  $T_3$  were considered in the range  $T_2$ - $T_5$  and, for each of them,  $T_4$  was let to vary in the interval  $T_3$ - $T_5$ . Each pair of the time intervals ( $T_3$ ,  $T_4$ ) was characterized in terms of purity, as shown in **Figure 6a**, and only those leading to  $P \geq P_{\text{spec}}$  were further evaluated in terms of yield. Most of the  $T_3$  values failed to satisfy  $P_{\text{spec}}$ , while some of them satisfied this constraint with multiple  $T_4$  values. For a  $T_3$  containing multiple  $T_4$  that were above  $P_{\text{spec}}$ , the highest  $T_4$  was always selected. In fact, the broader the collection interval, the higher the yield. For  $P_{\text{spec}} = 90\%$ , only three  $T_3$  values satisfied the condition  $P \geq P_{\text{spec}}$ , and for these points, the highest yield was achieved with the lowest  $T_3$ , as shown in **Figure 6b**. Therefore, the optimal point at  $T_{\text{load}} = 6.0$  min,  $T_{\text{elu}} = 20.0$  min and  $P_{\text{spec}}=90\%$  was given by the pair ( $T_3 = 26.5$  min,  $T_4 = 29.2$  min), characterized by 91.0% purity, 75.5% yield, and productivity of 2.55 g/L/h. If the constraint on purity was decreased to  $P_{\text{spec}} = 80\%$ , six values of  $T_3$  satisfied this condition, as shown in **Figure 6b**. The highest yield for  $P_{\text{spec}} = 80\%$  was for  $T_3 = 25.8$  min, and  $T_4 = 30.5$  min, leading to purity = 82.5%, yield = 91.1%, and productivity = 3.08 g/L/h.

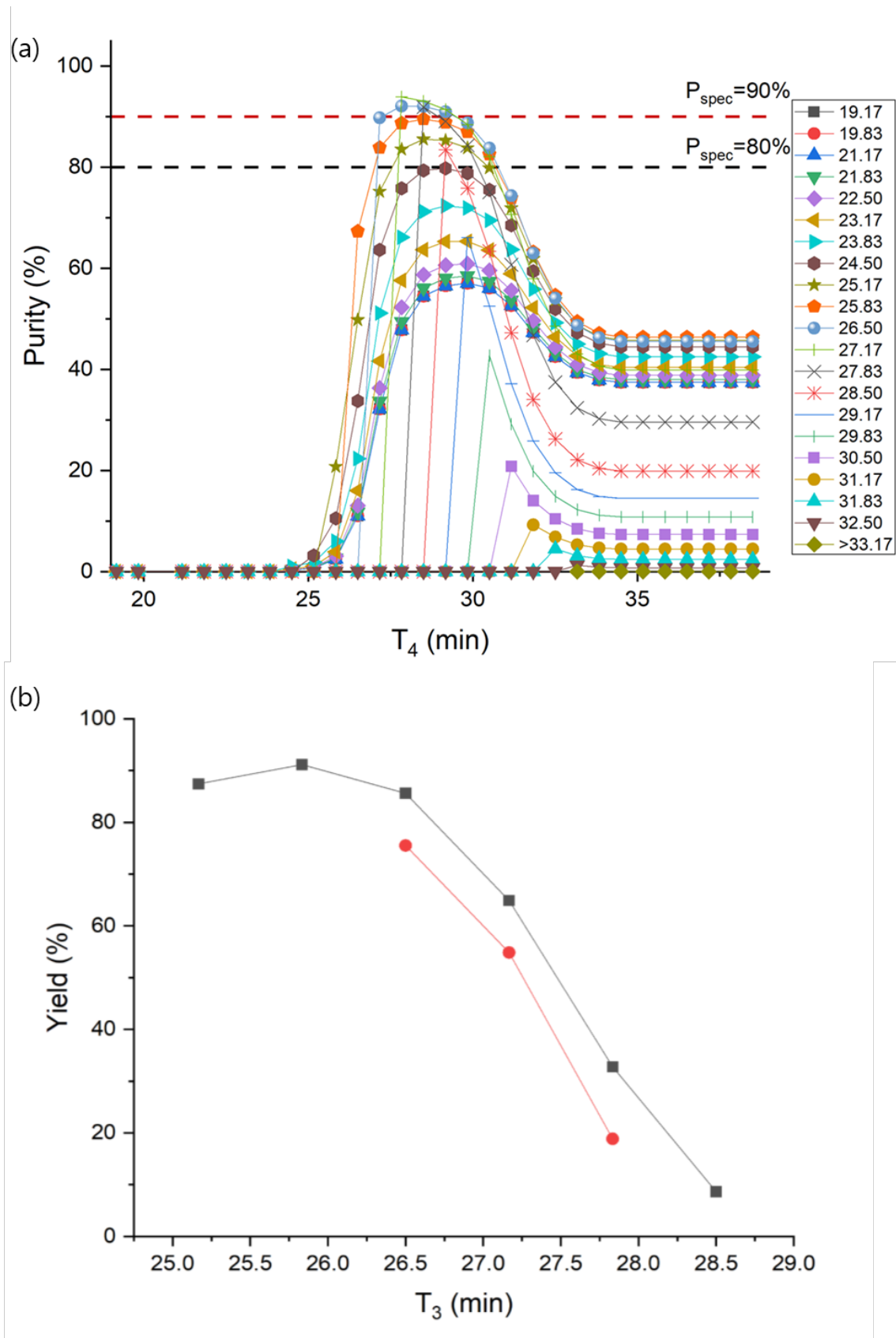


**Figure 6:** (a) Values of the target product purity as a function of  $T_4$  for various values of  $T_3$  and (b) yield as a function of  $T_3$  for  $P_{spec}$  equal to 90% (●), and 80% P (■).

A similar analysis was conducted for  $T_{\text{load}} = 6.0$  min and different values of  $T_{\text{elu}} = 10.0, 16.0, 24.0,$  and  $30.0$  min. For each of these times, the optimal point ( $T_3, T_4$ ) was determined as explained above, and the corresponding yield and productivity were reported in **Figure 7a** for  $P_{\text{spec}} = 90\%$  and in **Figure 7b** for  $P_{\text{spec}}=80\%$  (the corresponding optimal values of  $T_3$  and  $T_4$  are reported in **Table S1** and **S2**. In this case, it was not possible to define an optimal condition, but rather a Pareto front. It could be clearly observed that for a given  $P_{\text{spec}}$ , there is a trade-off between yield and productivity. In fact, by increasing  $T_{\text{elu}}$ , the W/P and P/S overlapping regions reduced due to a better separation of the components, while the productivity decreased. Therefore, high productivities could only be achieved at the expenses of the yield and vice versa.

Similar trends were observed for the different  $T_{\text{load}}$  considered, namely 6.0, 8.0, and 15.4 min. Indeed, an increase in the column loading led to more overlapping between the product and the impurities, thus determining an increasing difficulty in reaching the desired  $P_{\text{spec}}$ . In fact, for  $P_{\text{spec}} = 90\%$  and the highest  $T_{\text{load}} = 15.4$  min, only one optimal point, with respect to  $T_3$  and  $T_4$ , could be obtained and this was for the highest  $T_{\text{elu}}$ . Given this difficulty in the separation of the product, low yields were obtained at increasing  $T_{\text{load}}$ . On the other hand, since more protein is loaded onto the column the productivity increases. The Pareto fronts at different loading times somehow emerge from the data shown in **Figures 7a and 7b** for  $P_{\text{spec}} = 90$  and  $80\%$ , respectively. For  $P_{\text{spec}} = 90\%$ , the highest productivity was  $3.55$  g/L/hr, with  $T_{\text{load}} = 15.4$  min and  $T_{\text{elu}} = 30.0$  min. That is, the highest productivity was achieved with the maximum loading. The highest yield at  $84.6\%$  was reached for  $T_{\text{load}} = 6.0$  min and  $T_{\text{elu}} = 30.0$  min, indicating that, with the lowest loading and highest elution time, the smallest W/P and P/S fractions could be obtained, thus reaching the maximum yield. The Pareto front between yield and productivity is more evident for the results obtained with  $P_{\text{spec}} = 80\%$ , as all optimal values, with respect to  $T_3$  and  $T_4$ , for the batch purifications could be considered. The highest productivity was achieved with the maximum loading, while the highest yield was achieved with the lowest loading and the lowest elution gradient, with the exception of the yield value at  $T_{\text{load}} = 8.0$  min and  $T_{\text{elu}} = 24.0$  min.

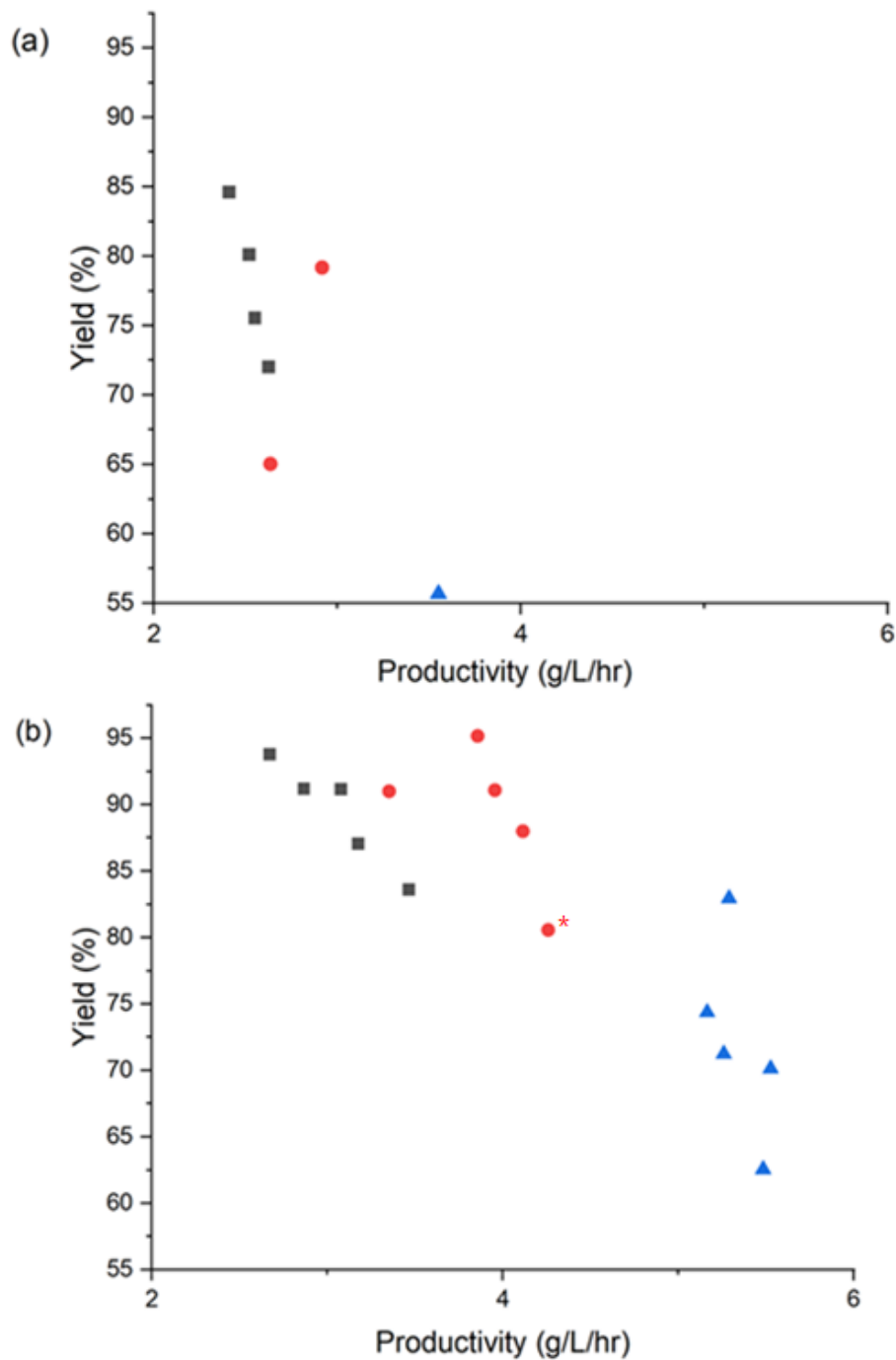


**Figure 7:** Optimal yield as function of productivity (a)  $P_{spec} = 90\%$  (b)  $P_{spec} = 80\%$ . The yield and productivity of  $T_{load} = 6.0$  min (■),  $T_{load} = 8.0$  min (●),  $T_{load} = 15.4$  min (▲) are found using the optimization method, with respect to  $T_3$  and  $T_4$ ,

Overall, using the developed ad hoc experimental design procedure, we were able to define the optimal conditions in terms of  $T_3$ ,  $T_4$ ,  $T_{elu}$  and  $T_{load}$  for the batch purification of PEGylated lysozyme, for a given purity specification, with a relatively small experimental effort.

### 3.4. MCSGP

The batch operation corresponding to  $T_{load} = 8.0$  min,  $T_{elu} = 10.0$  min and  $P_{spec} = 80\%$ , and shown in Figure 7b by a red asterisk, was selected to be transferred to the MCSGP unit with the aim of comparing, and possibly improving, purity, yield and productivity. The choice of the process with the minimum yield and maximum productivity among those with  $T_{load} = 8.0$  min was guided by the expectation that the MCSGP could, with its internal recycle of the W/P and P/S overlapping regions, lead to a significant improvement in the yield compared to the corresponding design batch. At the same time, the change in productivity could not be predicted *a priori*, and then it is reasonable to start from the process leading to its optimal value.

Using the same operating parameters, including the collection times  $T_3$  and  $T_4$ , the MCSGP was operated for 5 cycles and the corresponding UV chromatograms measured at the outlet of the first column are superimposed in **Figure 8**. As expected, the chromatogram of the first cycle, corresponding to the start-up phase, deviates the most from the others. On the other hand, after this first cycle, the good overlapping of the subsequent chromatograms suggests that cyclic steady state was reached. Compared to the batch process, the total time of a single MCSGP switch, which is the time needed to purify the given feed load, decreased from 46.0 min to 32.9 min, due to the advantage of utilizing two pumps and two columns for the process.

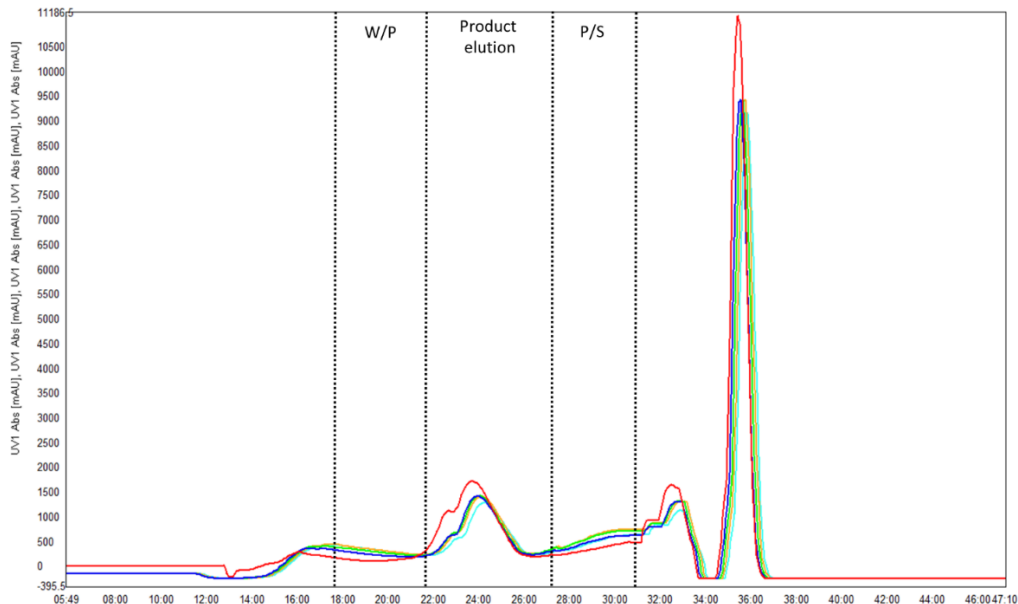


**Figure 8:** Superimposed CPX chromatograms of the MCSGP unit ( $T_{load} = 8.0$  min and  $T_{elu} = 10.0$  min). The UV absorbance at 280 nm at the outlet of the first column during the first ( ■ ), second ( ■ ), third ( ■ ), fourth ( ■ ) and fifth cycle ( ■ ) are represented.

**Table 6** summarizes the process performance for the 5 cycles of the MCSGP comparing them with the corresponding design batch. With  $T_{load} = 8.0$  min, in the start-up phase a relatively low yield of 66.6% but high purity of 88.2% were obtained. As the W/P and P/S recycling were calculated to last  $T_{load} = 0.4$  and 1.8 min, respectively, the subsequent switches were loaded with  $T_{load} = 5.8$  min to keep constant the amount of protein circulating inside the system. After the first switch, the process was already very close to steady state conditions. The average purity was 84.3%, which is comparable to that of the optimal design batch. At the same time, the product yield could be significantly improved from 79.6% of the design batch to 93.1%. This is mainly due to the internal recycling of the W/P and P/S regions, which were regarded as out-of-specification fractions and thus discarded in the design batch. Despite this increase in the yield and decrease of the total time of a single switch, the increase in the productivity was not significant, as the total load,  $T_{load}$  decreased. Overall, the implementation of the optimal batch process to MCSGP led to a significant increase in the product yield, which reached 93.1%, with a 13.5% gain with respect to the batch process. This increase in the yield also enabled to improve the productivity, despite a longer process. In fact, the productivity reached 4.30 g/L/h, with a gain of 0.09 g/L/h compared to batch.

**Table 6:** *Process performance for each switch of the MCSGP unit with  $T_{load} = 8.0$  min and  $T_{elu} = 10.0$  min*

Switch	Purity (%)	Yield (%)	Productivity (g/L/h)
1	88.2	66.6	4.10
2	85.4	95.6	4.27
3	84.5	92.8	4.15
4	80.3	92.6	4.14
5	84.1	95.5	4.27
6	85.8	99.4	4.44
7	82.5	98.2	4.39
8	84.8	100.1	4.47
9	83.8	96.1	4.29
10	84.4	99.0	4.43
11	82.9	97.8	4.37
Average	84.3	93.1	4.30
Batch	83.9	79.6	4.21

The MCSGP unit was also operated with  $T_{\text{elu}} = 20.0$  and  $30.0$  min with the same  $T_{\text{load}} = 8.0$  min (**Table S3** and **S4**). With these conditions, for both the gradient durations, the W/P and P/S recycles lasted  $T_{\text{load}} = 0.2$  and  $0.3$  min, respectively, and thus the fresh feed starting from the second switch was loaded for  $T_{\text{load}} = 7.5$  min. A summary of the process performance comparison between batch and MCSGP is shown in **Table 7**. For  $T_{\text{elu}} = 20.0$  min, while the purity remained comparable, the improvement in the yield was 2.8%, reaching 93.9%. Also the productivity had an improvement of 0.2 g/L/h, mainly attributed to the decreased  $T_{\text{total}}$ , which counterbalanced the decrease in  $T_{\text{load}}$  starting from the second switch. For  $T_{\text{elu}} = 30.0$  min, compared to the batch operation, the purity was comparable and the yield improvement was observed to be 2.0%, while the productivity decreased due to the increased  $T_{\text{total}}$  and decreased  $T_{\text{load}}$ . The increased  $T_{\text{total}}$  was attributed to the longer elution phase, in which the decreased flow rate for W/P and P/S recycles significantly increased the time of the elution phase in the MCSGP.

These considerations were summarized in the Pareto front for yield and productivity in the case of MCSGP shown in **Figure 9**. With the imposition of satisfying a  $P_{\text{spec}} = 80\%$ , we reached a clear compromise between product yield, which can be increased by prolonging the gradient duration, and productivity, improved by shortening the gradient. It is still worth noticing that this Pareto front for the MCSGP is quite flat at high yield, which can be significantly improved compared to that of the batch purification. This confirms that a periodically continuous process with automated internal recycle of the overlapping regions enables, at similar productivity, to recover most of the loaded product, avoiding wastes typical of a batch process.

**Table 7:** Summary of the performances of the MCSGP unit

$T_{\text{elu}}$ (min)	Purification method	$T_{\text{total}}$ (min)	Purity (%)	Yield (%)	Productivity (g/L/h)
10.0	Batch	46.0	83.9	79.6	4.21
	MCSGP	32.9	84.3	93.1	4.30
20.0	Batch	56.0	80.2	91.1	3.95
	MCSGP	52.2	81.5	93.9	4.15
30.0	Batch	66.0	82.0	91.0	3.35
	MCSGP	66.9	81.3	93.0	3.19

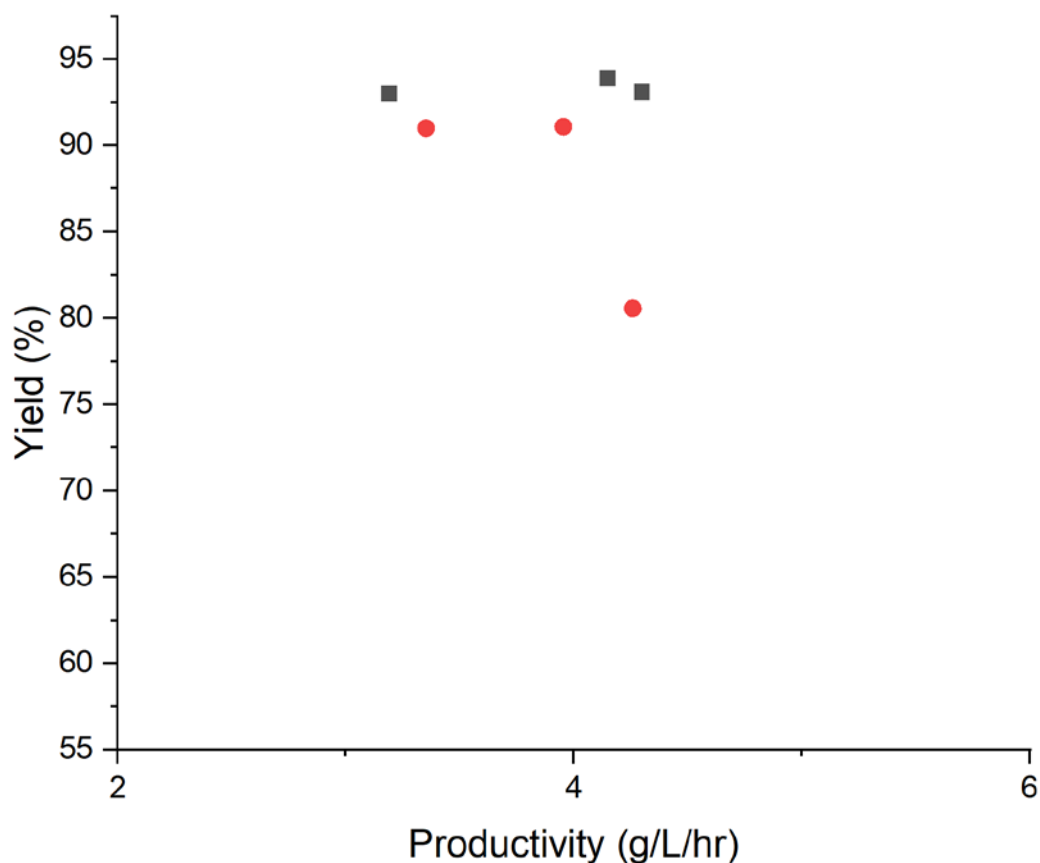


**Figure 9:** Comparison of yield as function of productivity for MCSGP (■) and batch purification (●) obtained through the developed optimization procedure for  $P_{spec} = 80\%$ .

#### 4. Conclusions

In this work, we developed an experimental procedure for the design of the operating conditions of a MCSGP unit, based on the *ad-hoc* optimization of the underlying batch design chromatogram. The procedure was illustrated through the purification of a PEGylated lysozyme mixture. This strategy aims at reaching optimal yield and productivity by varying 4 variables, namely  $T_{load}$ ,  $T_{elu}$ , and the collection times  $T_3$  and  $T_4$ , having as a constraint a minimum acceptable purity of the product pool ( $P_{spec}$ ). In the synthesized mPEG-lysozyme mixture, the proportion of the selected target product was 20.3%. Through suitable breakthrough experiments, which clearly demonstrated the competition among the different species in binding to the stationary phase, the DBC of each species was measured. Setting the OBC as 70% of the DBC,  $T_{load} = 15.4$  min was set as the maximum loading duration in the batch purification. With 30 fractions from each batch purification run, we considered different

hypothetical product pools by varying  $T_3$  and  $T_4$ , and for each  $T_{load}$  and  $T_{elu}$  we selected the collection interval leading to the maximum yield and satisfying the condition  $P \geq P_{spec}$ . The obtained results indicated a general trade-off between yield and productivity. With the highest  $T_{elu}$ , the yields were highest as higher  $T_{elu}$  decreased the overlapping regions of W/P and P/S and thus less target product was wasted in those fractions. At the same time, the productivity can be improved by lowering the run duration, and then decreasing  $T_{elu}$ . Regarding the loading, with the highest  $T_{load}$ , the highest productivities and lowest yields were observed, as, in contrast to the highest  $T_{elu}$ , the increased  $T_{load}$  increased the overlapping regions. From the Pareto front for the optimal batch purification at  $T_{load} = 8.0$  min we then selected 3 points ( $T_{elu} = 10.0, 20.0,$  and  $30.0$  min) to be translated to the MCSGP, while keeping the constraint  $P_{spec} = 80\%$ . For this periodically continuous process a yield-productivity trade-off was still in place. However, in this case the corresponding Pareto front is shifted towards higher yields ( $\geq 93.0\%$ ), with a marked improvement compared to the batch purification, as it is shown in **Figure 9**. Despite a slight increase in productivity, the internal recycle of the W/P and P/S overlapping regions typical of the MCSGP unit avoided discarding significant portions of out-of-specification product, thus improving the process yield.

### Supporting Information

The Supporting Information is available free of charge via the Internet at <http://pubs.acs.org/> and reports the  $^1\text{H-NMR}$  characterization of the intermediates for the synthesis of PEGylated lysozyme, the breakthrough curve, the optimal switching times for  $P_{spec}=80\%$  and  $90\%$  and the MCSGP performance parameters at  $T_{load}=8$  min and  $T_{elu}=20$  and  $30$  min.

### Declaration of Competing Interests

The authors declare no conflict of interests.

### References

- (1) Duncan R., Veronese F. Preface PEGylated protein conjugates: A new class of therapeutics for the 21st century. In: *PEGylated Protein Drugs: Basic Science and Clinical Applications*. Veronese FM (Ed.). Birkhäuser, Basel, Switzerland, **2009**. 1–9. [http://doi.org/10.1007/978-3-7643-8679-5\\_1](http://doi.org/10.1007/978-3-7643-8679-5_1).
- (2) Harris J., Chess R. Effect of pegylation on pharmaceuticals. *Nat Rev Drug Discov*, **2003**, *2*, 214–221. <https://doi.org/10.1038/nrd1033>.
- (3) Freitas Dda S., Abrahão-Neto J. Biochemical and biophysical characterization of lysozyme

- modified by PEGylation. *Int J Pharm.* **2010**, 392(1-2):111-7. <https://doi.org/10.1016/j.ijpharm.2010.03.036>.
- (4) Market Data Forecast. Global PEGylated Proteins Market Size, Share, Trends and Growth Analysis Report – Segmented By Protein Type, Services, Application, Consumables, End-User and Region - Industry Forecast | 2020 to 2025, *Market Data Forecast*, **2020**. <https://www.marketdataforecast.com/market-reports/pegylated-proteins-market>.
  - (5) Fee C.J. Protein conjugates purification and characterization. In: *PEGylated Protein Drugs: Basic Science and Clinical Applications*. Veronese FM (Ed.). Birkhäuser, Basel, Switzerland, **2009**. 113-126. [https://doi.org/10.1007/978-3-7643-8679-5\\_7](https://doi.org/10.1007/978-3-7643-8679-5_7).
  - (6) Luca C., Felletti S., Lievore G., Buratti A., Vogg S., Morbidelli M., Cavazzini A., Catani M., Macis M., Ricci A., Cabri W. From batch to continuous chromatographic purification of a therapeutic peptide through multicolumn countercurrent solvent gradient purification. *J Chromatogr A.* **2020**, 1625; <https://doi.org/10.1016/j.chroma.2020.461304>.
  - (7) Moosmann A, Christel J, Boettinger H, Mueller E. Analytical and preparative separation of PEGylated lysozyme for the characterization of chromatography media. *J Chromatogr A.* **2010**, 1217(2), 209-15. <https://doi.org/10.1016/j.chroma.2009.11.031>.
  - (8) Pabst T.M., Buckley J.J., Ramasubramanyan N., and Hunter A.K. Comparison of strong anion-exchangers for the purification of a PEGylated protein. *J Chromatogr A.* **2007**, 1147(2), 172–82. <https://doi.org/10.1016/j.chroma.2007.02.051>.
  - (9) Brumeanu T.-D., Zaghouani H., and Bona C. Purification of antigenized immunoglobulins derivatized with monomethoxypolyethylene glycol. *J Chromatogr A.* **1995**, 696, 219–25. [https://doi.org/10.1016/0021-9673\(94\)01275-j](https://doi.org/10.1016/0021-9673(94)01275-j).
  - (10) Fee C.J. and Van Alstine J.M. PEG-proteins: Reaction engineering and separation issues. *Chem. Eng. Sci.* **2006**, 61 (3), 924–39. <https://doi.org/10.1016/j.ces.2005.04.040>.
  - (11) Esposito P., Barbero L., Caccia P., Caliceti P., D’Antonio M., Piquet G., Veronese F. Pegylation of growth hormone-releasing hormone GRF analogues. *Adv. Drug Deliv. Rev.* **2003**, 55(10), 1279–91. [https://doi.org/10.1016/S0169-409X\(03\)00109-1](https://doi.org/10.1016/S0169-409X(03)00109-1).
  - (12) Ströhlein G., Aumann L., Mazzotti M., Morbidelli M., A continuous, counter-current multi-column chromatographic process incorporating modifier gradients for ternary separations. *J. Chromatogr. A.* **2006**, 1126, 338– 346. <https://doi.org/10.1016/j.chroma.2006.05.011>.
  - (13) Jungbauer A. Continuous downstream processing of biopharmaceuticals. *Trends Biotechnol.* **2013**, 31, 479– 492. <https://doi.org/10.1016/j.tibtech.2013.05.011>.
  - (14) Krättli M., Müller-Späth T., Morbidelli M., Multifraction separation in countercurrent chromatography (MCSGP). *Biotechnol. Bioeng.* **2013**, 110, 2436–44.

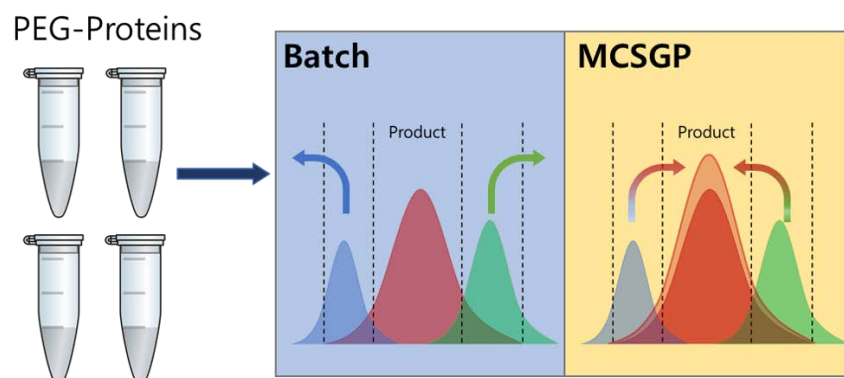
<https://doi.org/10.1002/bit.24901>.

- (15) Aumann L., Morbidelli M., A continuous multicolumn countercurrent solvent gradient purification (MCSGP) process. *Biotechnol. Bioeng.* **2007**, 98, 1043–55. <https://doi.org/10.1002/bit.21527>.
- (16) Steinebach F., Müller-Späth T., Morbidelli M. Continuous counter-current chromatography for capture and polishing steps in biopharmaceutical production, *Biotech. J.* **2016**, 11, 1126–41. <https://doi.org/10.1002/biot.201500354>.
- (17) Pfister D., Nicoud L., Morbidelli, M. Continuous biopharmaceutical processes: chromatography, bioconjugation, and protein stability. Cambridge: Cambridge University Press. **2018**, 153-202. <https://doi:10.1017/9781108332897>
- (18) Vogg S., Muller-Spath T., Morbidelli M. Design space and robustness analysis of batch and counter-current frontal chromatography processes for the removal of antibody aggregates. *J. Chromatogr. A.* **2020**, 1619. 460943. <https://doi.org/10.1016/j.chroma.2020.460943>.
- (19) Baur D., Angarita M., Müller-Späth T., Steinebach F., Morbidelli M. Comparison of batch and continuous multi-column protein A capture processes by optimal design. *Biotechnol J.* **2016**, 11(7), 920-31. <https://doi.org/10.1002/biot.201500481>.
- (20) Müller-Späth T., Ströhlein G., Lyngberg O., Maclean D. Enabling high purities and yields in therapeutic peptide purification using multicolumn countercurrent solvent gradient purification. *Chem. Today.* **2013**. 31. 56–60.
- (21) Aumann L., Morbidelli M. A semicontinuous 3-column countercurrent solvent gradient purification (MCSGP) process. *Biotechnol Bioeng.* **2008**, 99(3), 728-33. <https://doi.org/10.1002/bit.21585>. PMID: 17680681.
- (22) De Luca C., Felletti S., Lievore G., Chenet T., Morbidelli M., Sponchioni M., Cavazzini A., Catani M. Modern trends in downstream processing of biotherapeutics through continuous chromatography: The potential of Multicolumn Countercurrent Solvent Gradient Purification. *Trends Anal. Chem.* **2020**, 132:116051. <https://doi.org/10.1016/j.trac.2020.116051>
- (23) Bigelow E., Song Y., Chen J., Holstein M., Huang Y., Duhamel L., Stone K., Furman R., Li Z. J., Ghose S. Using continuous chromatography methodology to achieve high-productivity and high-purity enrichment of charge variants for analytical characterization. *J. Chromatogr. A.* **2021**, 1643. 462008. <https://doi.org/10.1016/j.chroma.2021.462008>.
- (24) Roberts M.J., Bentley M.D., Harris J.M. Chemistry for peptide and protein PEGylation. *Adv Drug Deliv Rev.* **2002**, 54(4), 459-76. [https://doi.org/10.1016/s0169-409x\(02\)00022-4](https://doi.org/10.1016/s0169-409x(02)00022-4).
- (25) Kateja, N., Nitika, Dureja, S., Rathore, A.S. Development of an integrated continuous PEGylation and purification process for granulocyte colony stimulating factor. *J. Biotechnol.*

**2020**, 322, 79-89. <https://doi.org/10.1016/j.jbiotec.2020.07.008>.

- (26) Ulmer, N., Pfister, D., Morbidelli, M. Reactive separation processes for the production of PEGylated proteins. *Curr Opin Colloid Interface Sci.* **2017**, 31, 86-91. <https://doi.org/10.1016/j.cocis.2017.09.003>.
- (27) Zydney, A.L. Continuous downstream processing for high value biological products: A Review. *Biotechnol Bioeng.* **2016**, 113(3), 465-75. <https://doi.org/10.1002/bit.25695>.

**For Table of Contents only**



A design procedure is developed for the multicolumn countercurrent solvent gradient purification (MCSGP) of PEGylated lysozyme, highlighting optimal conditions improving the batch separation.